Supporting Information

Selective Recognition of D-Aldohexoses by Boronic Acid-Functionalized Molecularly Imprinted Cross-Linked Micelles

Joseph K. Awino, Roshan W. Gunasekara, and Yan Zhao*

Department of Chemistry, Iowa State University, Ames, Iowa 50011-3111, USA

Table of Contents

General Method

Routine ^{1}H and ^{13}C NMR spectra were recorded on a Bruker DRX-400, on a Bruker AV II 600 or on a Varian VXR-400 spectrometer. ESI-MS mass was recorded on Shimadzu LCMS-2010 mass spectrometer. Dynamic light scattering (DLS) data were recorded at 25 °C using PDDLS/ CoolBatch 90T with PD2000DLS instrument. Isothermal titration calorimetry (ITC) was performed using a MicroCal VP-ITC Microcalorimeter with Origin 7 software and VPViewer2000 (GE Healthcare, Northampton, MA).

Scheme 1S

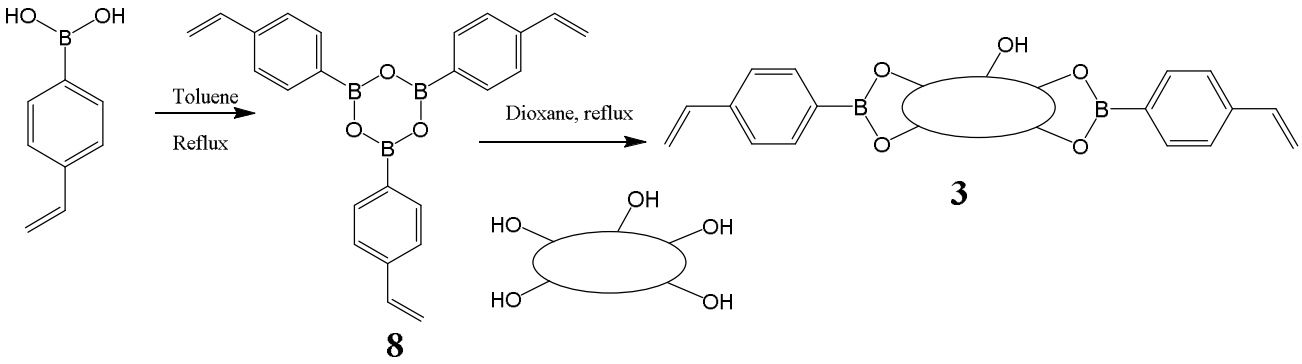

Syntheses

Compounds **8**[1] and **9**[2] were synthesized following reported procedures.

Compound 8. 4-Vinylphenylboronic acid (1.00 g, 6.80 mmol) was refluxed in a Dean-Stark apparatus with 100 mL of toluene until water no longer evolved. Evaporation of the toluene to a volume of 10 mL led to the deposition of 0.84 g of pale tan crystals of tris(4-vinylpheny1)boroxine. Recrystallization of a small sample of the product from toluene afforded colorless powder.

Compound 9. α-D-Glucose (102 mg, 0.57 mmol) and tris(4-vinylpheny1)boroxine (150 mg, 0.38 mmol) were mixed in 50 mL of dioxane. The azeotrope was distilled for 3 h, and the remaining solvent was evaporated in vacuum. The product was recrystallized from toluene to yield white crystalline solid (118 mg, 77%).

Synthesis of MINPs. MINPs were synthesized according to previously reported procedures.[3] To a micellar solution of surfactant **1** (9.3 mg, 0.02 mmol) in D_2O (2.0 mL), divinylbenzene (DVB, 2.8 µL, 0.02 mmol), **9** in DMSO (10 µL of a solution of 16.2 mg/mL, 0.0004 mmol), and 2,2-dimethoxy-2-phenylacetophenone (DMPA) in DMSO (10 µL of a 12.8 mg/mL, 0.0005 mmol) were added. The

[1] Hoffmann, A.K.; Thomas W.M., *J. Am. Chem. Soc.*, **1959**, *81*, 580.
[2] (a) Wulff, G.; Schauhoff, S. *J. Org. Chem.* **1991**, *56*, 395. (b) Norrild, J.C.; Eggert, H., *J. Am. Chem. Soc.*, **1995**, *117*, 1479.
[3] Awino, J. K.; Zhao, Y. *J. Am. Chem. Soc.* **2013**, *135*, 12552.

mixture was ultrasonicated for 10 min. Compound **2** (4.1 mg, 0.024 mmol), $CuCl_2$ in D_2O (10 µL of 6.7 mg/mL, 0.0005 mmol), and sodium ascorbate in D_2O (10 µL of 99 mg/mL, 0.005 mmol) were then added and the reaction mixture was stirred slowly at room temperature for 12 h. Compound **3** (10.6 mg, 0.04 mmol), $CuCl_2$ (10 µL of a 6.7 mg/mL solution in D_2O, 0.0005 mmol), and sodium ascorbate (10 µL of a 99 mg/mL solution in D_2O, 0.005 mmol) were then added and the solution stirred for another 6 h at room temperature. The reaction mixture was transferred to a glass vial, purged with nitrogen for 15 min, sealed with a rubber stopper, and irradiated in a Rayonet reactor for 12 h. ^{1}H NMR spectroscopy was used to monitor the progress of reaction. The reaction mixture was poured into acetone (8 mL). The precipitate was collected by centrifugation and washed with a mixture of methanol/acetic acid (5 mL/0.1 mL) three times. The off white product was dried in air to afford the final MINPs in quantitative yield (> 80%).

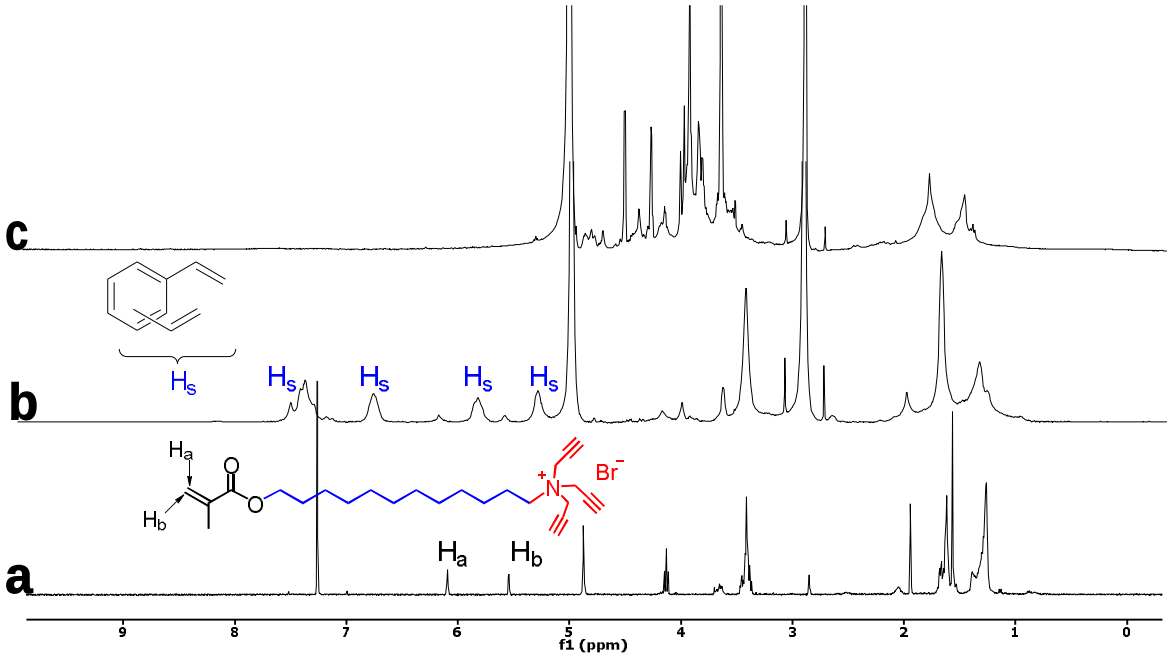

Figure 1S. ^{1}H NMR spectra of (a) **1** in $CDCl_3$, (b) alkynyl-SCM in D_2O, and (c) MINP(glucose) in D_2O.

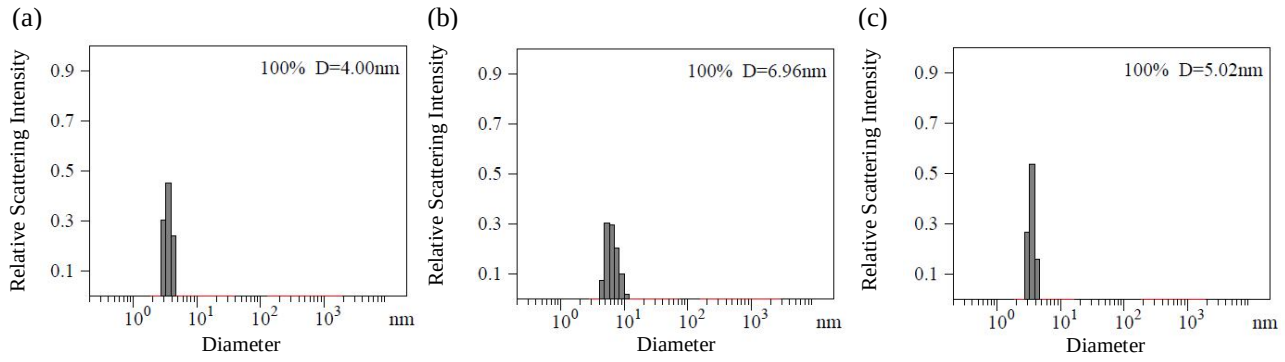

Figure 2S. Distribution of the hydrodynamic diameters of the nanoparticles in water as determined by DLS for (a) alkynyl-SCM, (b) surface-functionalized SCM, and (c) MINP(glucose) after purification.

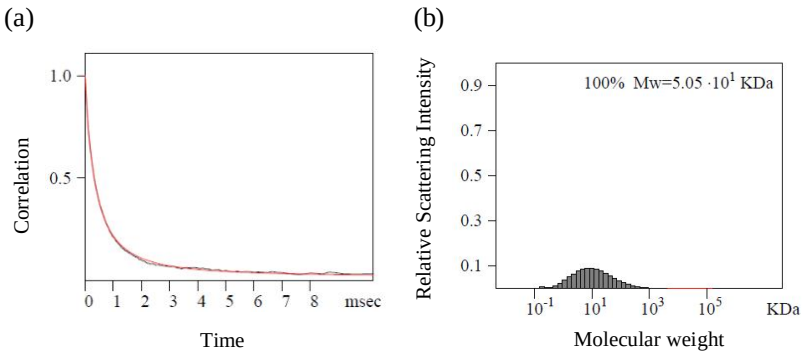

Figure 3S. The correlation curve and the distribution of the molecular weight for MINP(glucose) from the DLS. The PRECISION DECONVOLVE program assumes the intensity of scattering is proportional to the mass of the particle squared. If each unit of building block for the MINP(glucose) is assumed to contain one molecule of compound **1** (MW = 465 g/mol), 1.2 molecules of compound **2** (MW = 172 g/mol), one molecule of DVB (MW = 130 g/mol), 0.8 molecules of compound **3** (MW = 264 g/mol), and 0.04 molecules of 4-vinylphenylboronic acid (MW = 148 g/mol), the molecular weight of MINP(glucose) translates to 50 [= 50500 / (465 + 1.2×172 + 130 + 0.8×264 + 0.04×148)] of such units.

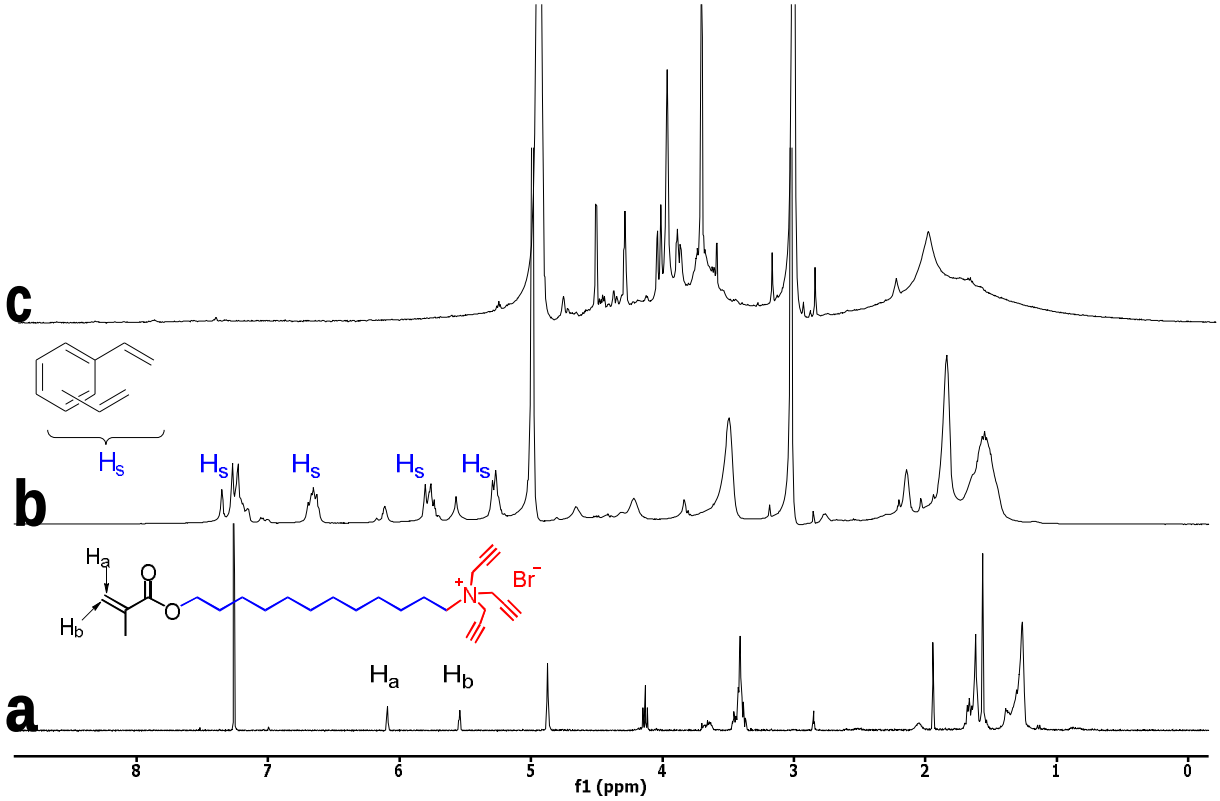

Figure 4S. ^{1}H NMR spectra of (a) **1** in $CDCl_3$, (b) alkynyl-SCM in D_2O, and (c) MINP(mannose) in D_2O.

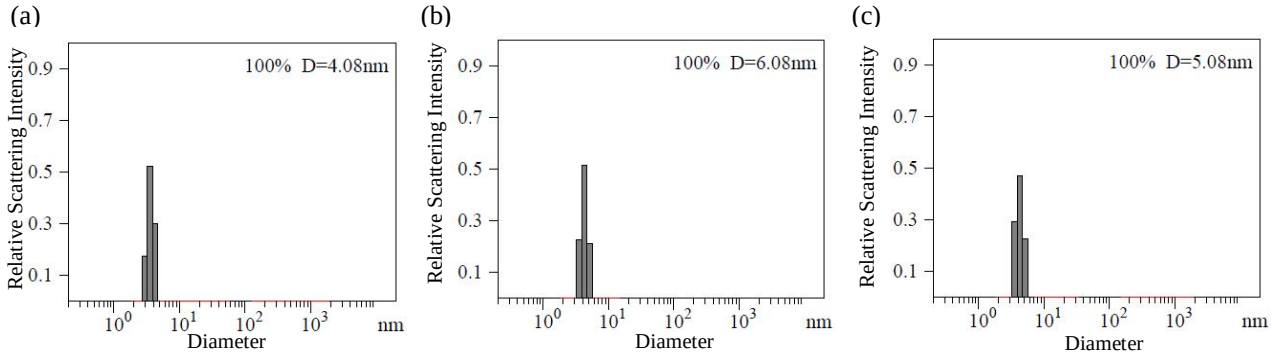

Figure 5S. Distribution of the hydrodynamic diameters of the nanoparticles in water as determined by DLS for (a) alkynyl-SCM, (b) surface-functionalized SCM, and (c) MINP(mannose) after purification.

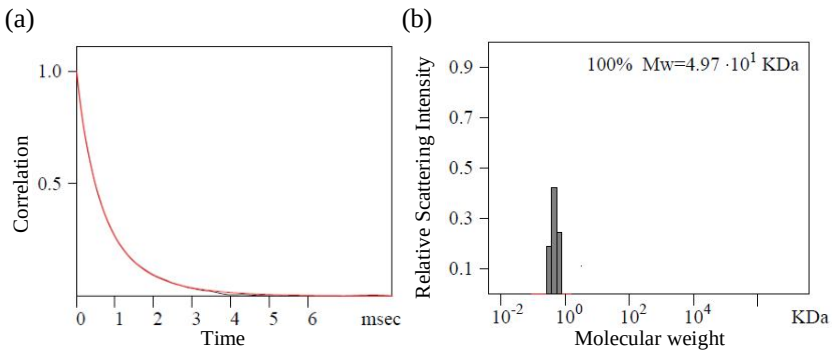

Figure 6S. The correlation curve and the distribution of the molecular weight for MINP(mannose) from the DLS. The PRECISION DECONVOLVE program assumes the intensity of scattering is proportional to the mass of the particle squared. If each unit of building block for the MINP(mannose) is assumed to contain one molecule of compound **1** (MW = 465 g/mol), 1.2 molecules of compound **2** (MW = 172 g/mol), one molecule of DVB (MW = 130 g/mol), 0.8 molecules of compound **3** (MW = 264 g/mol), and 0.04 molecules of 4-vinylphenylboronic acid (MW = 148 g/mol), the molecular weight of MINP(mannose) translates to 49 [= 49700 / (465 + 1.2×172 + 130 + 0.8×264 + 0.04×148)] of such units.

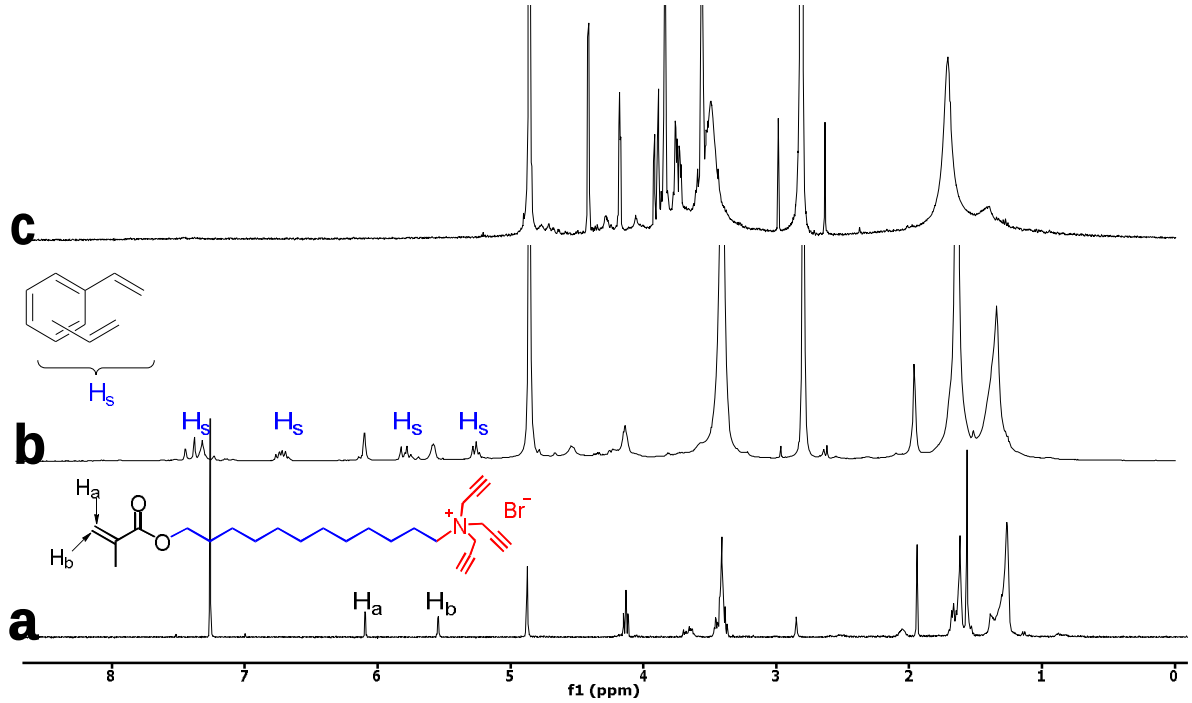

Figure 7S. ^{1}H NMR spectra of (a) **1** in $CDCl_3$, (b) alkynyl-SCM in D_2O, and (c) MINP(**5**) in D_2O.

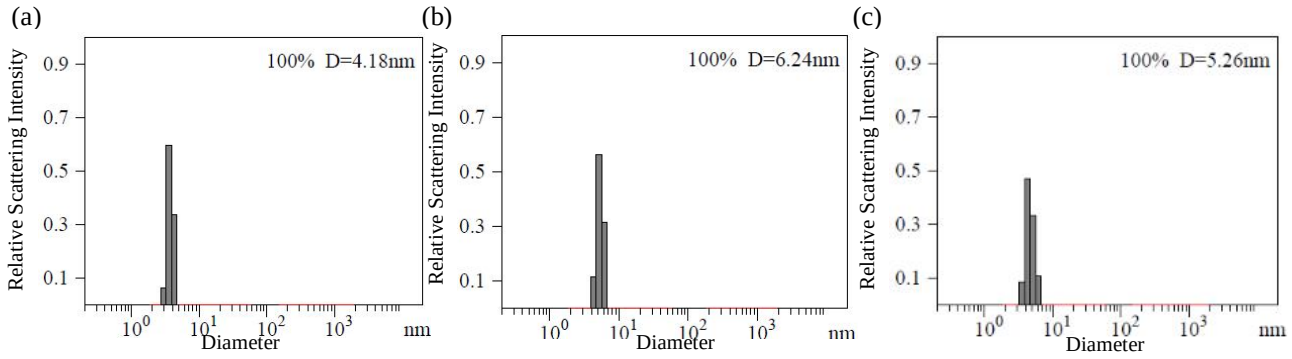

Figure 8S. Distribution of the hydrodynamic diameters of the nanoparticles in water as determined by DLS for (a) alkynyl-SCM, (b) surface-functionalized SCM, and (c) MINP(**5**) after purification.

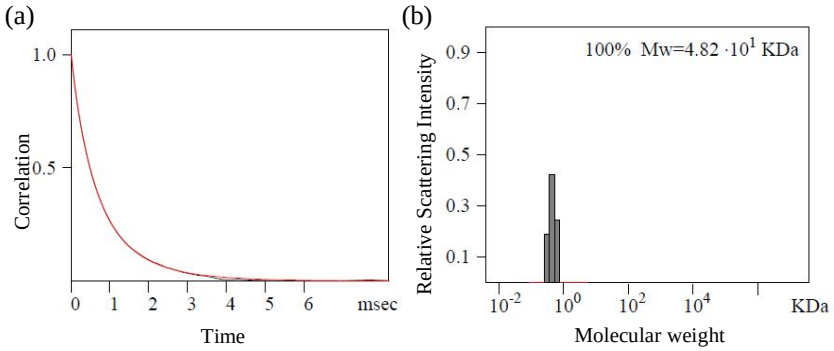

Figure 9S. The correlation curve and the distribution of the molecular weight for MINP(**5**) from the DLS. The PRECISION DECONVOLVE program assumes the intensity of scattering is proportional to the mass of the particle squared. If each unit of building block for the MINP(**5**) is assumed to contain one molecule of compound **1** (MW = 465 g/mol), 1.2 molecules of compound **2** (MW = 172 g/mol), one molecule of DVB (MW = 130 g/mol), 0.8 molecules of compound **3** (MW = 264 g/mol), and 0.04 molecules of 4-vinylphenylboronic acid (MW = 148 g/mol), the molecular weight of MINP(**5**) translates to 47 [= 48200 / (465 + 1.2×172 + 130 + 0.8×264 + 0.04×148)] of such units.

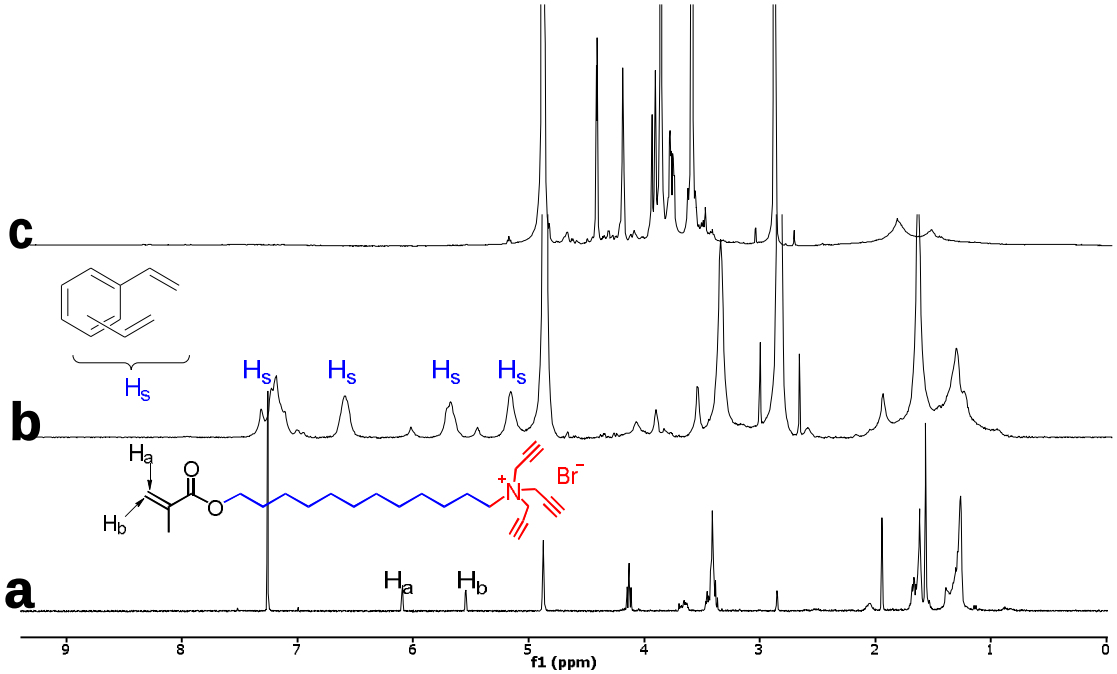

Figure 10S. ^{1}H NMR spectra of (a) **1** in $CDCl_3$, (b) alkynyl-SCM in D_2O, and (c) MINP(galactose) in D_2O.

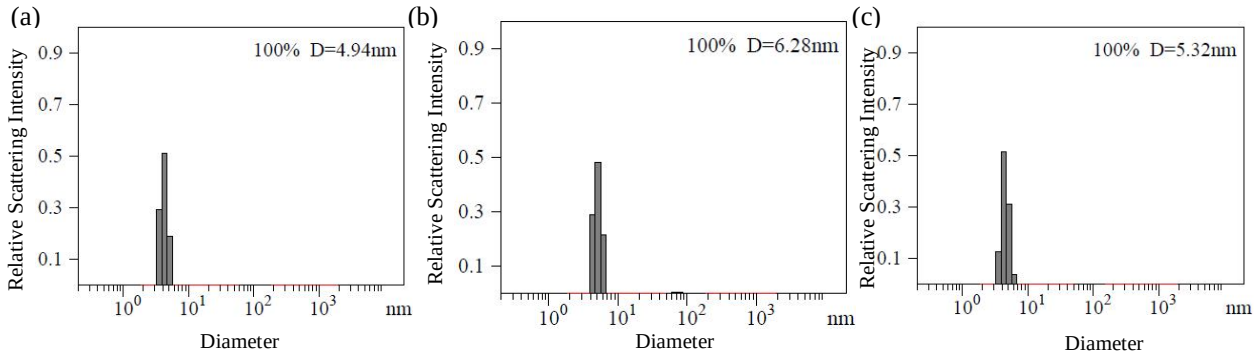

Figure 11S. Distribution of the hydrodynamic diameters of the nanoparticles in water as determined by DLS for (a) alkynyl-SCM, (b) surface-functionalized SCM, and (c) MINP(galactose) after purification.

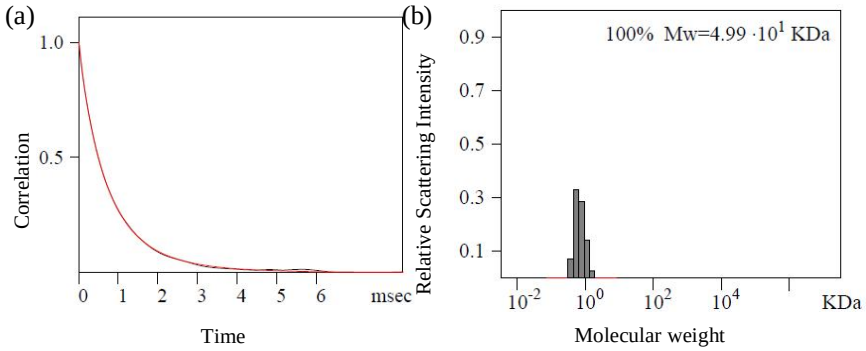

Figure 12S. The correlation curve and the distribution of the molecular weight for MINP(galactose). from the DLS. The PRECISION DECONVOLVE program assumes the intensity of scattering is proportional to the mass of the particle squared. If each unit of building block for the MINP(galactose) is assumed to contain one molecule of compound **1** (MW = 465 g/mol), 1.2 molecules of compound **2** (MW = 172 g/mol), one molecule of DVB (MW = 130 g/mol), 0.8 molecules of compound **3** (MW = 264 g/mol), and 0.04 molecules of 4-vinylphenylboronic acid (MW = 148 g/mol), the molecular weight of MINP(galactose) translates to 49 [= 49900 / (465 + 1.2×172 + 130 + 0.8×264 + 0.04×148)] of such units.

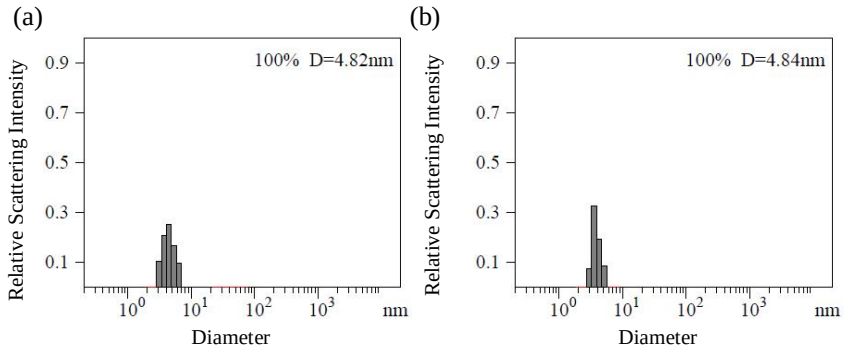

Figure 13S. Distribution of the hydrodynamic diameters of the nanoparticles in water as determined by DLS (a) before adding galactose to the MINP(galactose). (b) after adding galactose to the MINP(galactose).

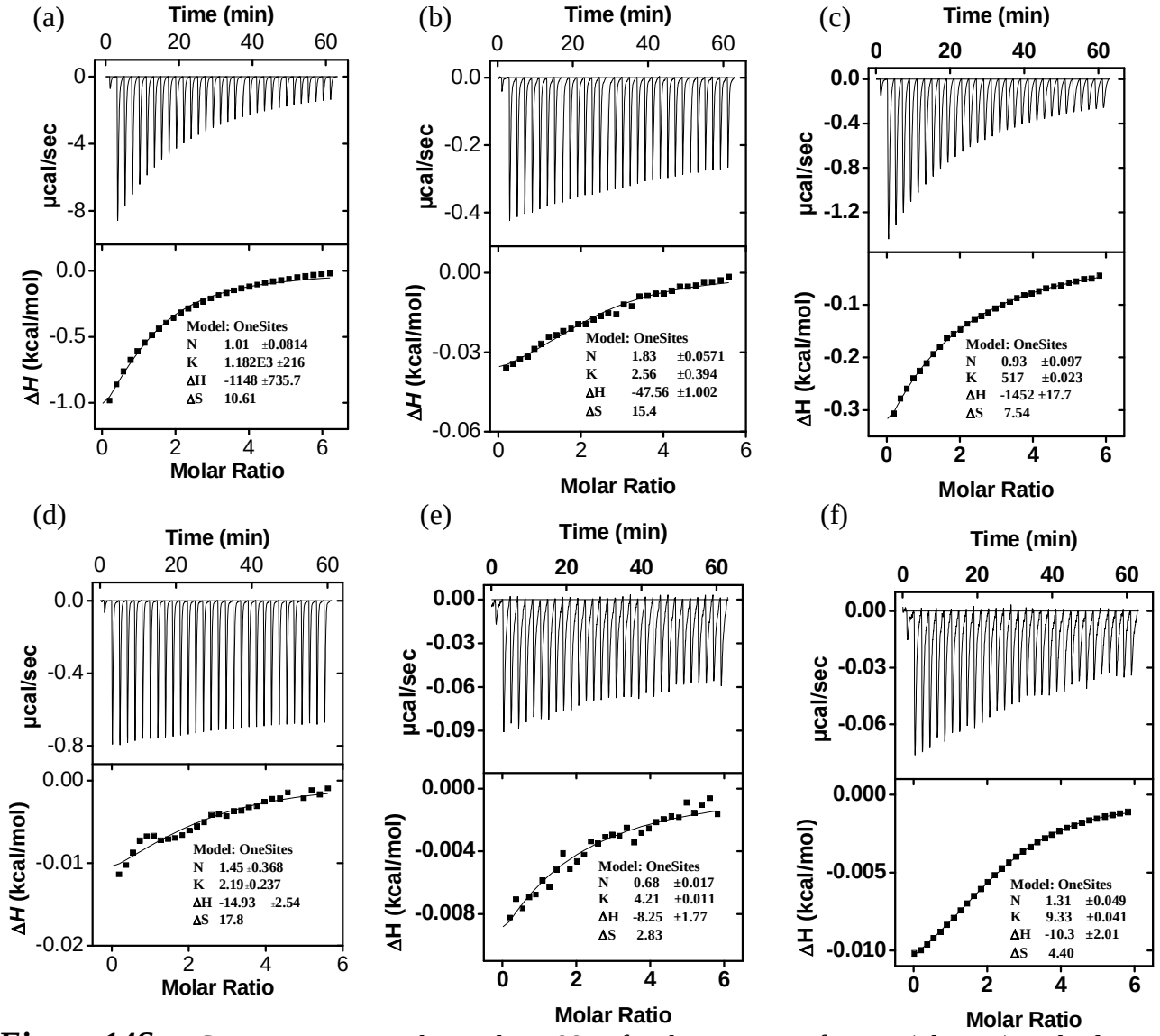

Figure 14S. ITC titration curves obtained at 298 K for the titration of MINP(glucose) with glucose (a), mannose (b), allose (c), galactose (d), altrose (e), and gulose (f) in 10 mM HEPES buffer (pH 7.4). The data correspond to entries 1–6, respectively, in Table 1. The top panel shows the raw calorimetric data. The area under each peak represents the amount of heat generated at each ejection and is plotted against the molar ratio of MINP to the substrate. The solid line is the best fit of the experimental data to the sequential binding of N equal and independent binding sites on the MINP. The heat of dilution for the substrate, obtained by adding the substrate to the buffer, was subtracted from the heat released during the binding. Binding parameters were auto-generated after curve fitting using Microcal Origin 7.

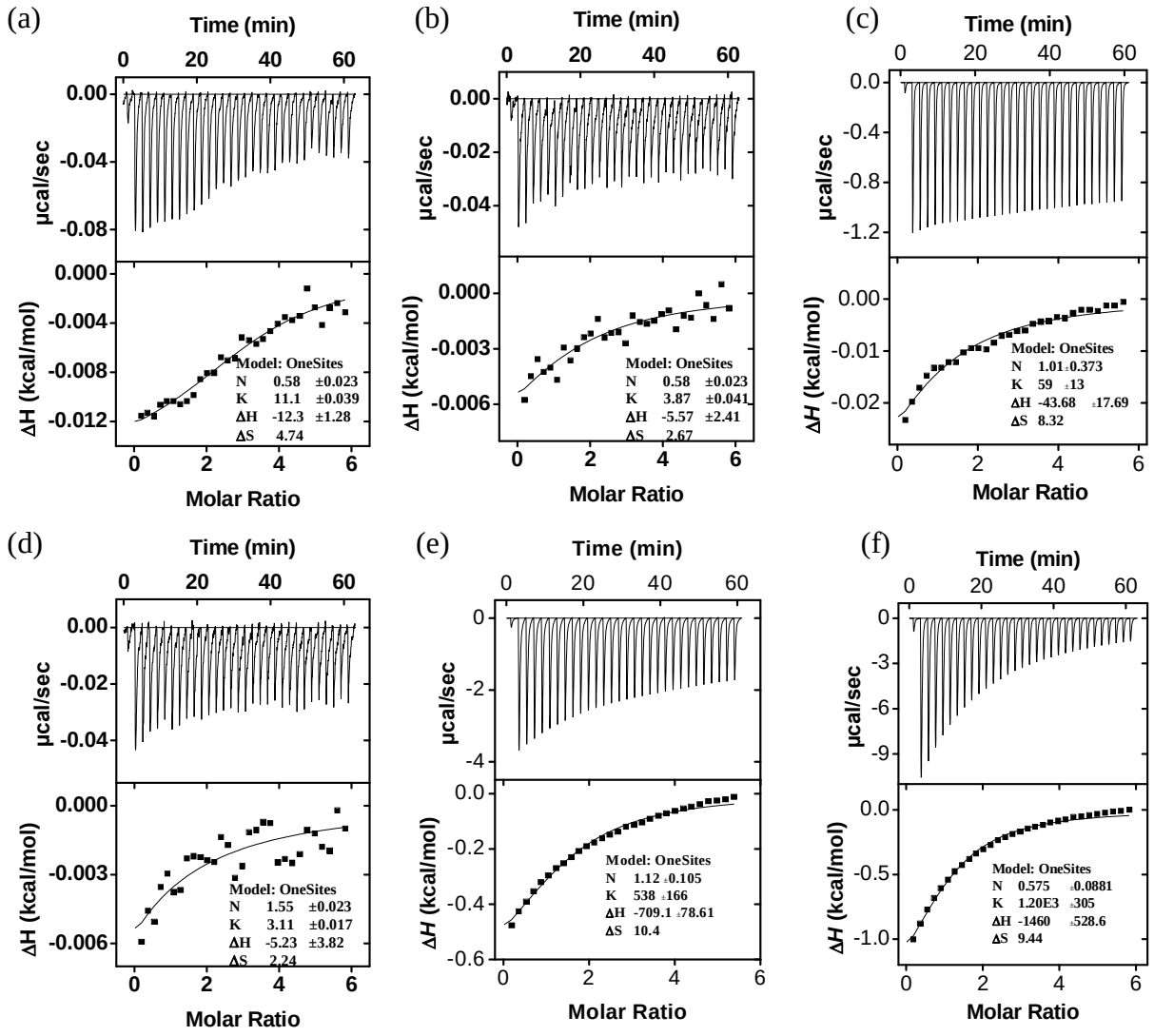

Figure 15S. ITC titration curves obtained at 298 K for the titration of MINP(glucose) with talose (a), idose (b), fructose (c), xylose (d) at pH 7.4, glucose at pH 6.5 (e), and glucose at pH 8.5 (f) in 10 mM HEPES buffer. The data correspond to entries 7–12, respectively, in Table 1. The top panel shows the raw calorimetric data. The area under each peak represents the amount of heat generated at each ejection and is plotted against the molar ratio of MINP to the substrate. The solid line is the best fit of the experimental data to the sequential binding of N equal and independent binding sites on the MINP. The heat of dilution for the substrate, obtained by adding the substrate to the buffer, was subtracted from the heat released during the binding. Binding parameters were auto-generated after curve fitting using Microcal Origin 7.

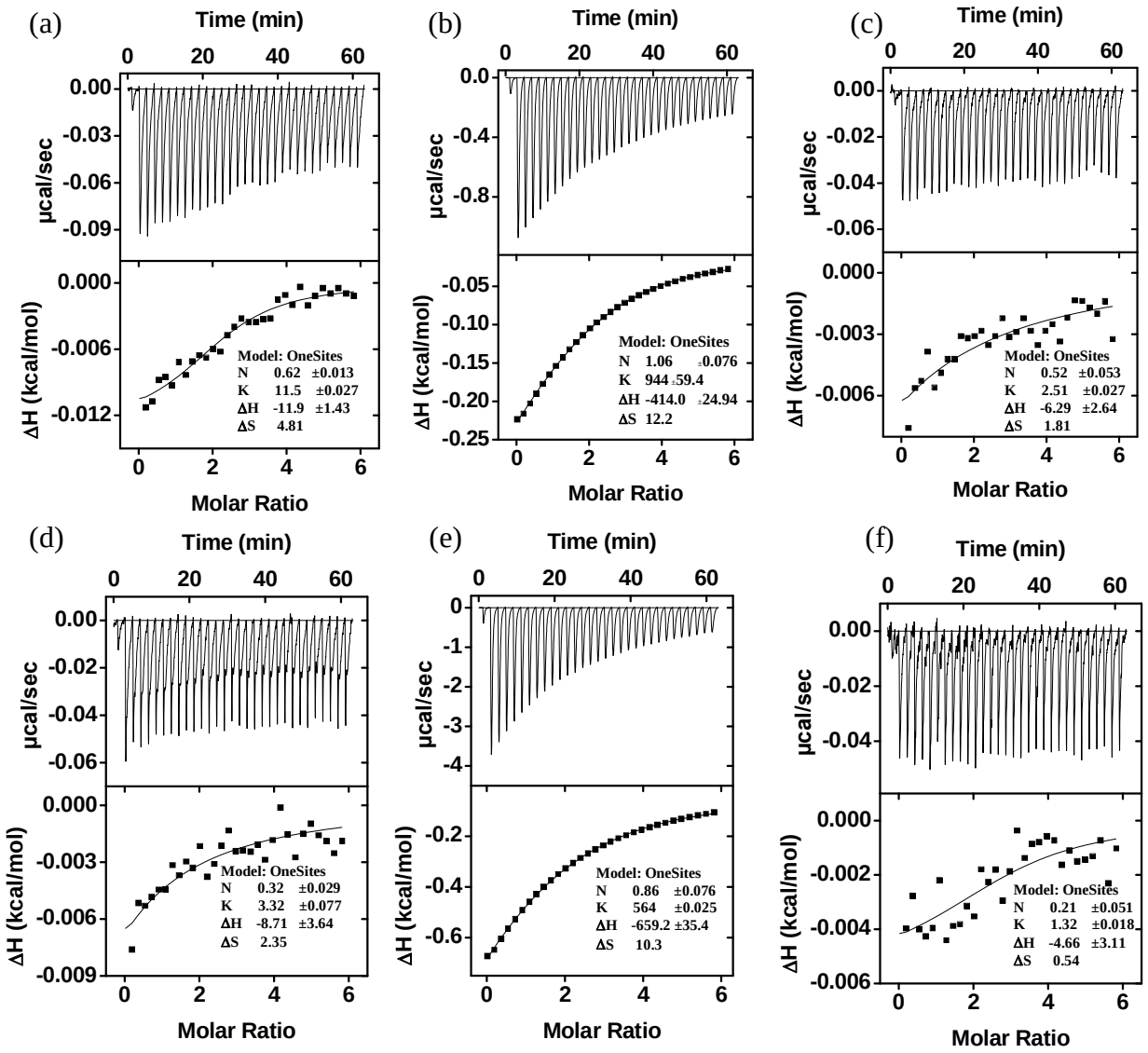

Figure 16S. ITC titration curves obtained at 298 K for the titration of MINP(mannose) with glucose (a), mannose (b), allose (c), galactose (d), altrose (e), and gulose (f) in 10 mM HEPES buffer (pH 7.4). The data correspond to entries 13–18, respectively, in Table 1. The top panel shows the raw calorimetric data. The area under each peak represents the amount of heat generated at each ejection and is plotted against the molar ratio of MINP to the substrate. The solid line is the best fit of the experimental data to the sequential binding of N equal and independent binding sites on the MINP. The heat of dilution for the substrate, obtained by adding the substrate to the buffer, was subtracted from the heat released during the binding. Binding parameters were auto-generated after curve fitting using Microcal Origin 7.

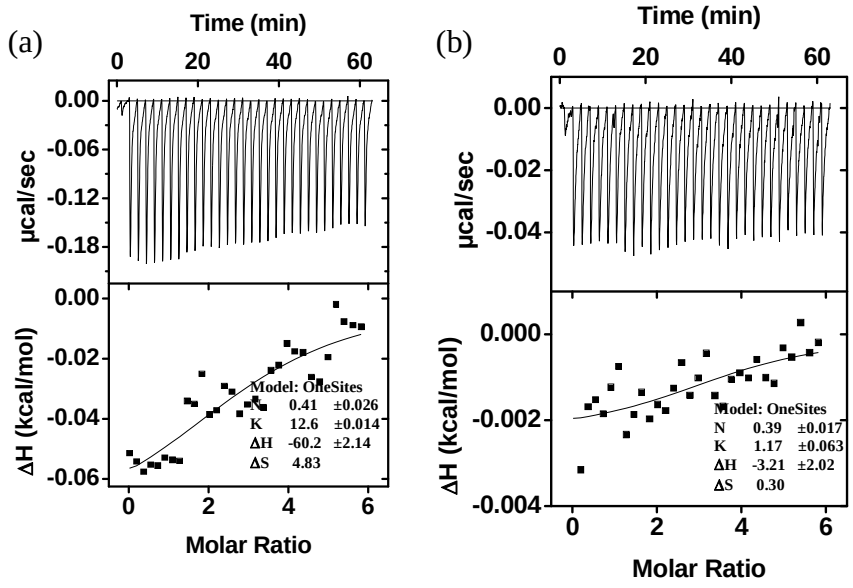

Figure 17S. ITC titration curves obtained at 298 K for the titration of MINP(mannose) with talose (a) and idose (b) in 10 mM HEPES buffer (pH 7.4). The data correspond to entries 19–20, respectively, in Table 1. The top panel shows the raw calorimetric data. The area under each peak represents the amount of heat generated at each ejection and is plotted against the molar ratio of MINP to the substrate. The solid line is the best fit of the experimental data to the sequential binding of N equal and independent binding sites on the MINP. The heat of dilution for the substrate, obtained by adding the substrate to the buffer, was subtracted from the heat released during the binding. Binding parameters were auto-generated after curve fitting using Microcal Origin 7.

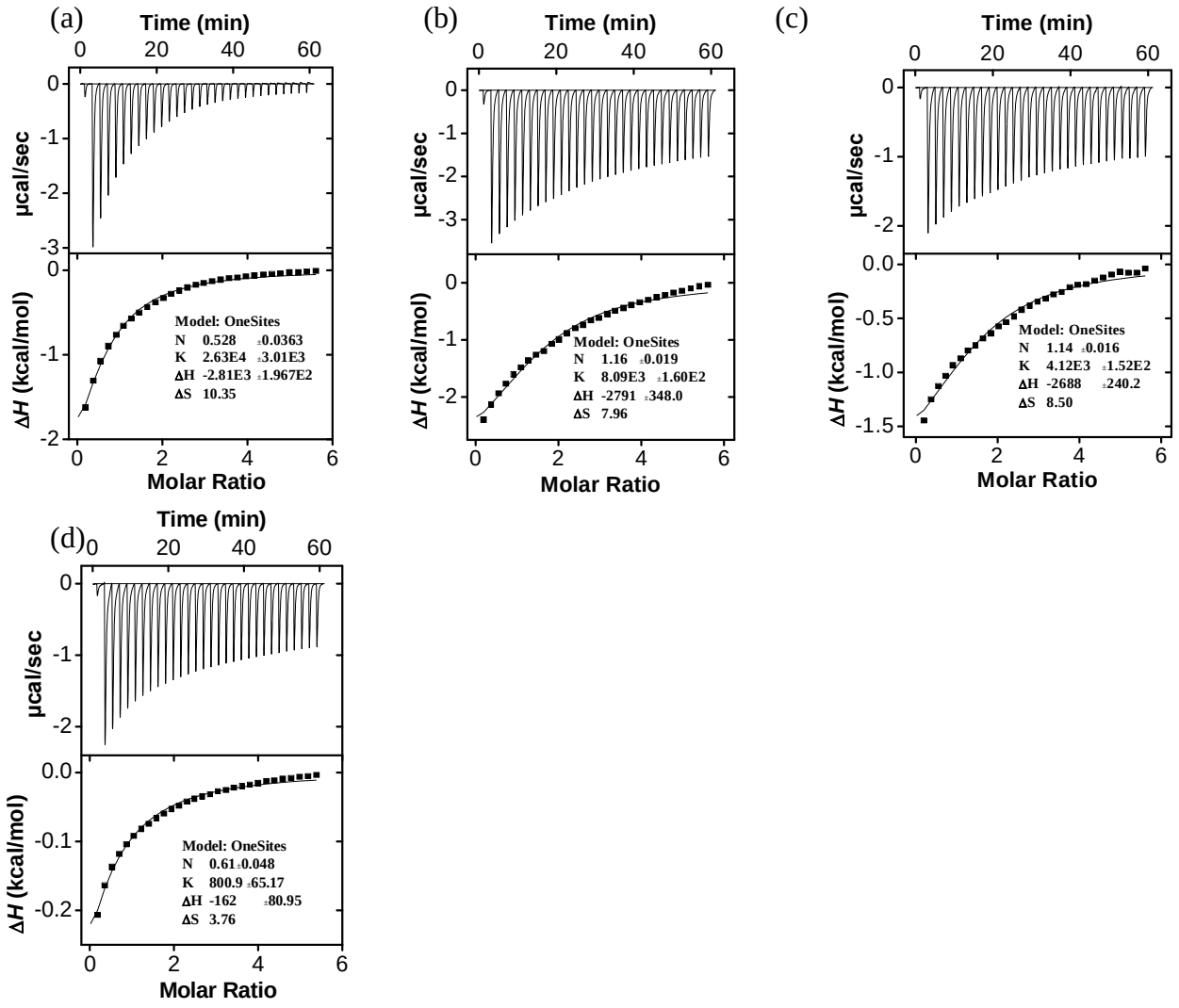

Figure 18S. ITC titration curves obtained at 298 K for the titration of MINP(**5**) with **5** (a), **6** (b), **7** (c), and mannose (d) in 10 mM HEPES buffer (pH 7.4). The data correspond to entries 21–24, respectively, in Table 1. The top panel shows the raw calorimetric data. The area under each peak represents the amount of heat generated at each ejection and is plotted against the molar ratio of MINP to the substrate. The solid line is the best fit of the experimental data to the sequential binding of N equal and independent binding sites on the MINP. The heat of dilution for the substrate, obtained by adding the substrate to the buffer, was subtracted from the heat released during the binding. Binding parameters were auto-generated after curve fitting using Microcal Origin 7.

Table 1S. ITC binding data for boronic acid-functionalized MINPs[a].

Entry	Host	Guest	K_a (10^3 M^{-1})	-Δ*G* (kcal/mol)	N
1	MINP(galactose)	glucose	0.004[b]	--[b]	--[b]
2	MINP(galactose)	mannose	0.001[b]	--[b]	--[b]
3	MINP(galactose)	allose	0.011[b]	--[b]	--[b]
4	MINP(galactose)	galactose	1.41 ± 0.16	4.3	0.9 ± 0.1
5	MINP(galactose)	altrose	0.029[b]	--[b]	--[b]
6	MINP(galactose)	gulose	0.80 ± 0.04	4.0	1.2 ± 0.1
7	MINP(galactose)	talose	0.017[b]	--[b]	--[b]
8	MINP(galactose)	idose	0.011[b]	--[b]	--[b]
9	MINP(galactose)[c]	galactose	1.49 ± 0.08	4.3	1.0 ± 0.1
10	MINP(galactose)[d]	galactose	1.48 ± 0.06	4.3	1.0 ± 0.1
11	MINP(galactose)[e]	galactose	1.42 ± 0.03	4.3	1.0 ± 0.1

[a] The titrations were performed in 10 mM HEPES buffer at pH 7.4. [b] Binding was extremely weak. Because the binding constant was estimated from ITC, -Δ*G* and *N* are not listed. [c] The titration was performed in following conditions. Volume delivered: 10 μL, Volume delivering time: 7.1 s, Spacing time: 120 s. [d] The titration was performed in following conditions. Volume delivered: 10 μL, Volume delivering time: 10 s, Spacing time: 120 s. [e] The titration was performed in following conditions. Volume delivered: 10 μL, Volume delivering time: 10 s, Spacing time: 240 s.

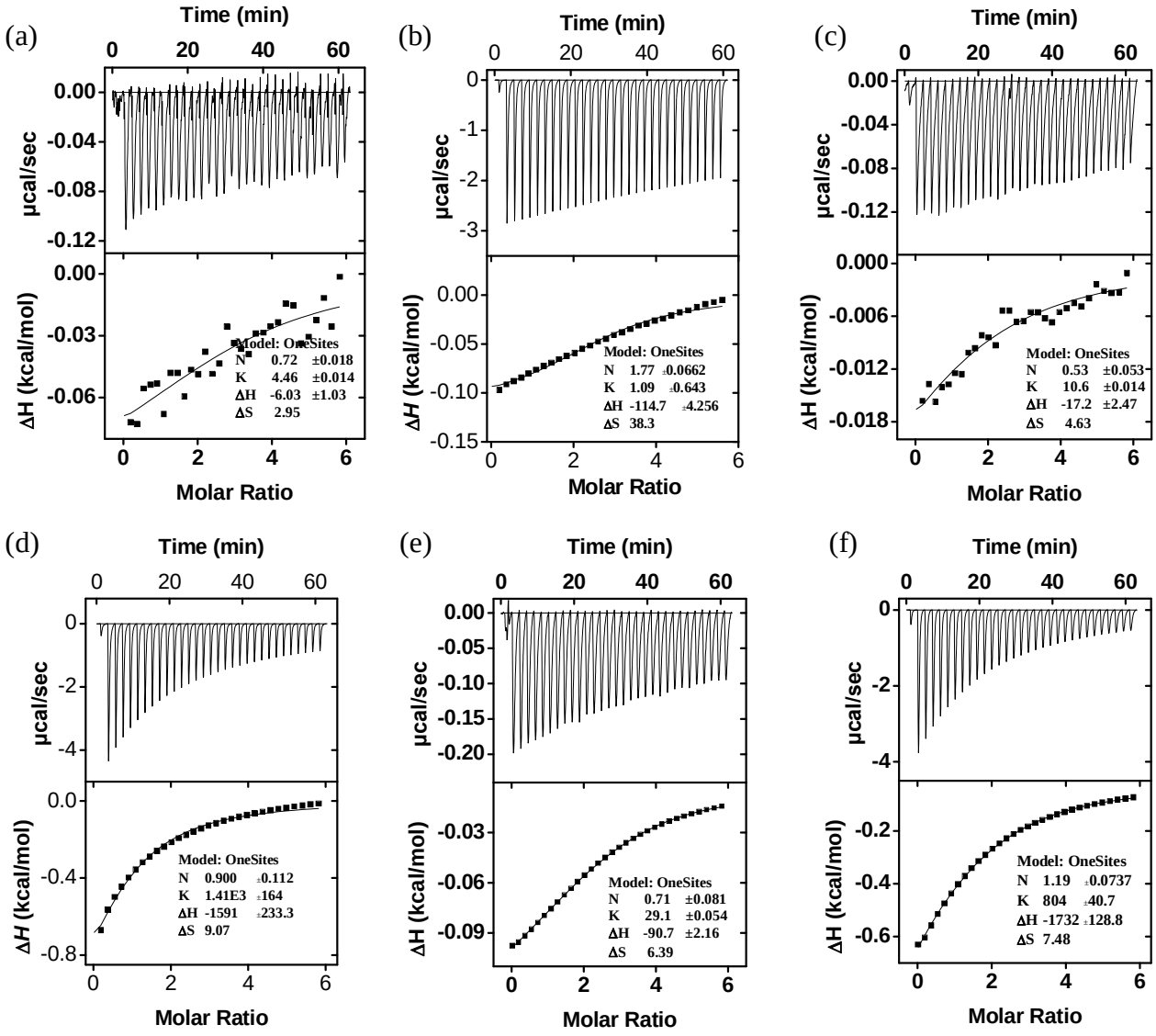

Figure 19S. ITC titration curves obtained at 298 K for the titration of MINP(galactose) with glucose (a), mannose (b), allose (c), galactose (d), altrose (e), and gulose (f) in 10 mM HEPES buffer (pH 7.4). The data correspond to entries 1–8, respectively, in Table 1S. The top panel shows the raw calorimetric data. The area under each peak represents the amount of heat generated at each ejection and is plotted against the molar ratio of MINP to the substrate. The solid line is the best fit of the experimental data to the sequential binding of N equal and independent binding sites on the MINP. The heat of dilution for the substrate, obtained by adding the substrate to the buffer, was subtracted from the heat released during the binding. Binding parameters were auto-generated after curve fitting using Microcal Origin 7.

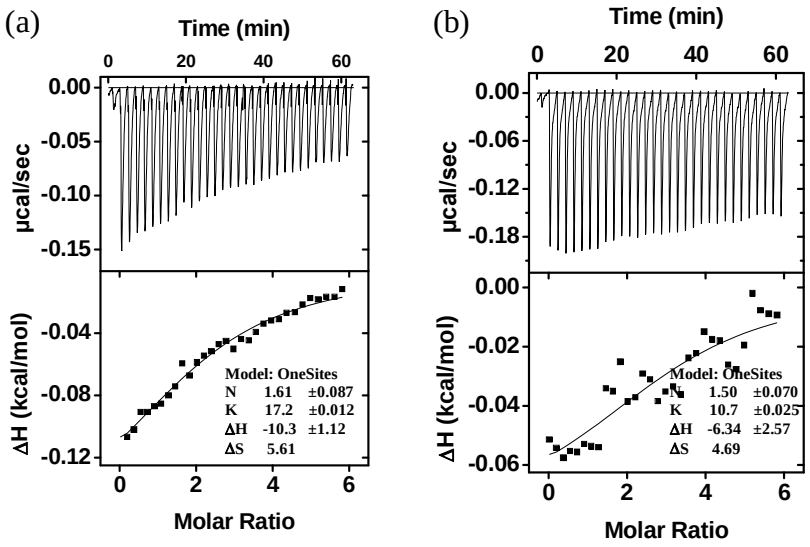

Figure 20S. ITC titration curves obtained at 298 K for the titration of MINP(galactose) with talose (a) and idose (b) in 10 mM HEPES buffer (pH 7.4). The data correspond to entries 7 and 8 respectively, in Table 1S. The top panel shows the raw calorimetric data. The area under each peak represents the amount of heat generated at each ejection and is plotted against the molar ratio of MINP to the substrate. The solid line is the best fit of the experimental data to the sequential binding of N equal and independent binding sites on the MINP. The heat of dilution for the substrate, obtained by adding the substrate to the buffer, was subtracted from the heat released during the binding. Binding parameters were auto-generated after curve fitting using Microcal Origin 7.

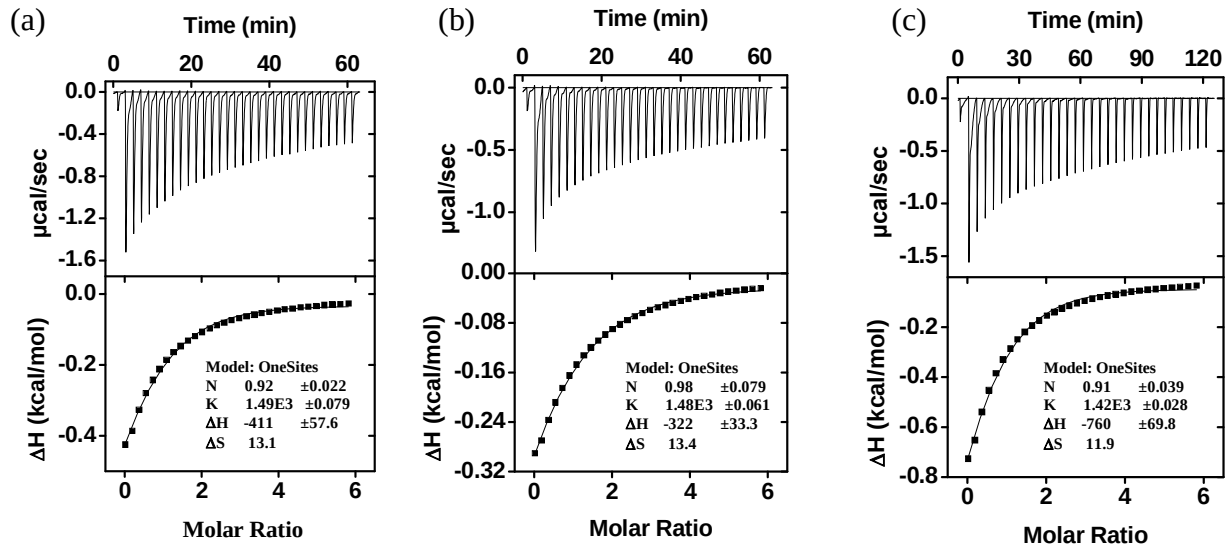

Volume delivered : 10 µL	Volume delivered : 10 µL	Volume delivered : 10 µL
Volume delivering time: 7.1 s	Volume delivering time: 10 s	Volume delivering time: 10 s
Spacing time : 120 s	Spacing time : 120 s	Spacing time : 240 s

Figure 21S. ITC titration curves obtained at 298 K for the titration of MINP(galactose) with galactose (a), galactose (b), and galactose (c) in 10 mM HEPES buffer (pH 7.4). The data correspond to entries 9–11, respectively, in Table 1S. The top panel shows the raw calorimetric data. The area under each peak represents the amount of heat generated at each ejection and is plotted against the molar ratio of MINP to the substrate. The solid line is the best fit of the experimental data to the sequential binding of N equal and independent binding sites on the MINP. The heat of dilution for the substrate, obtained by adding the substrate to the buffer, was subtracted from the heat released during the binding. Binding parameters were auto-generated after curve fitting using Microcal Origin 7.

[1]H NMR spectra

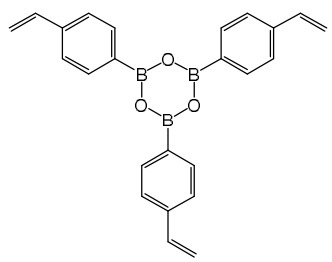

8

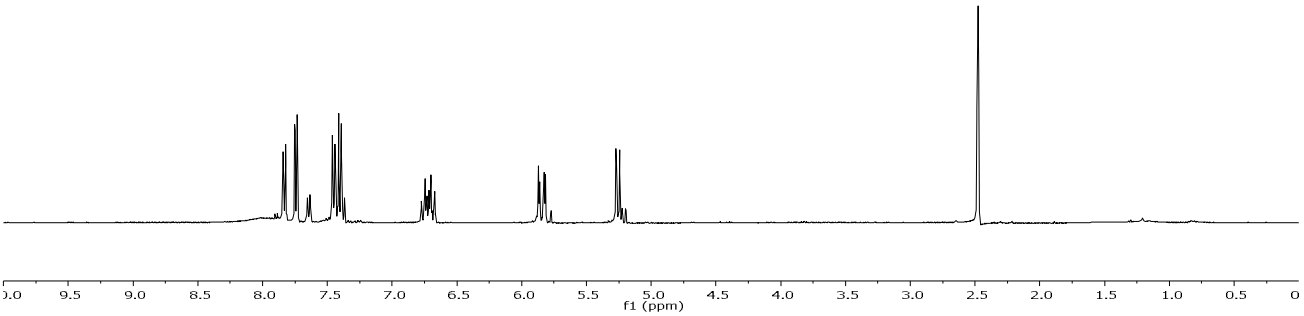

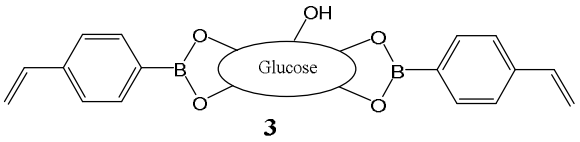

3

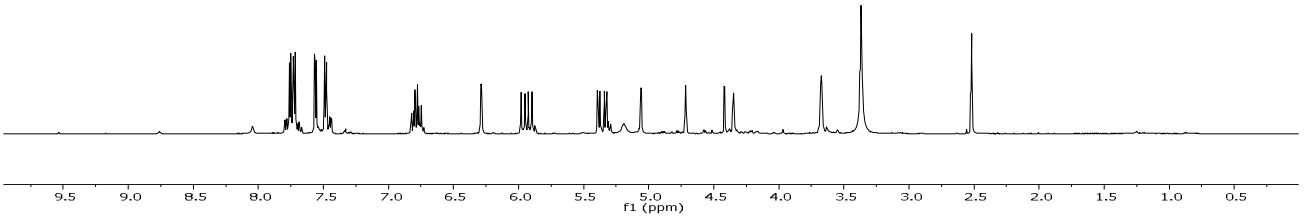

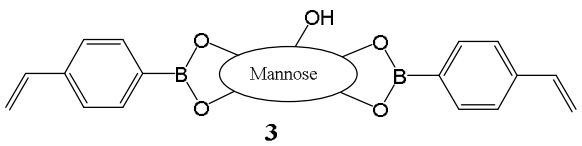

3

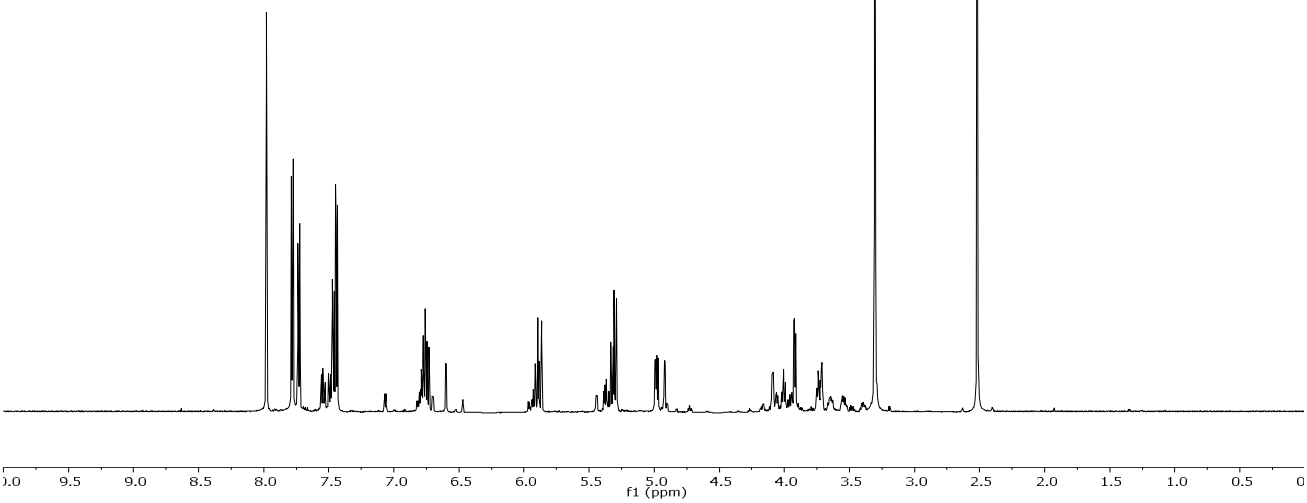

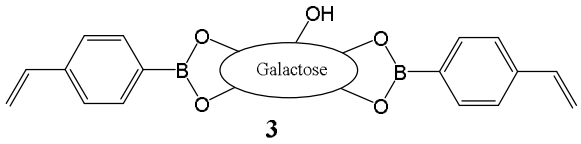

3